Inorg. Chem. **2003**, *42*, 5660–5668

Covalent Linkage of the Type-2 and Type-3 Structural Mimics to Model the Active Site Structure of Multicopper Oxidases: Synthesis and Magneto- Structural Properties of Two Angular Trinuclear Copper(II) Complexes

Arindam Mukherjee,[†] Indranil Rudra,[‡] Sunil G. Naik,[†] Suryanarayanasastry Ramasesha,[‡,§] Munirathinam Nethaji,[†] and Akhil R. Chakravarty*[,†]

Department of Inorganic and Physical Chemistry, and Solid State and Structural Chemistry Unit, Indian Institute of Science, Bangalore-560012, India

Received May 26, 2003

Two new angular trinuclear copper(II) complexes of formulation $[Cu_3(HL)LL']$$(ClO_4)$, where L′ is imidazole (Him, **1**) or 1-methylimidazole (1-MeIm, **2**) and H_3L is a Schiff base obtained from the condensation of salicylaldehyde and 1,3-diaminopropan-2-ol (2:1 mole ratio), are prepared from a reaction of $[Cu_2L(\mu\text{-Br})]$ and [Cu(HL)] in the presence of L′ and isolated as perchlorate salts. The crystal structures of **1** and **2** consist of a trinuclear copper(II) unit formed by the covalent linkage of monomeric type-2 mimic and dimeric type-3 mimic precursor complexes to give an angular arrangement of the metal atoms in the core which is a model for the active site structure of blue multicopper oxidases. In **1** and **2**, the coordination geometry of two terminal copper atoms is distorted square-planar. The central copper has a distorted square-pyramidal (4 + 1) geometry. The mean Cu···Cu distance is ∼3.3 Å. The complex has a diphenoxo-bridged dicopper(II) unit with the phenoxo oxygen atoms showing a planar geometry. In addition, the complex has an endogenous alkoxo-bridged dicopper(II) unit showing a pyramidal geometry for the oxygen atom. The 1:1 electrolytic complexes show a d–d band at 607 nm. Cyclic voltammetry of the complexes in MeCN containing 0.1 M TBAP using a glassy carbon working electrode displays a Cu_3(II)/Cu_2(II)Cu(I) couple near –1.0 V (vs SCE). The variable temperature magnetic susceptibility measurements in the range 300–18 K show antiferromagnetic coupling in the complexes giving magnetic moments of ∼3.0 μ_B at 300 K and ∼2.1 μ_B at 18 K for the tricopper(II) unit. The experimental susceptibility data are theoretically fitted using a model with Heisenberg spin-$^1/_2$ Hamiltonian for a trimer of spin-$^1/_2$ copper(II) ions having two exchange parameters involving the alkoxo-bridged dicopper(II) ($J1$) and the diphenoxo-bridged dicopper(II) ($J2$) units, giving $J1$ and $J2$ values of –82.7, –73 cm^{-1} for **1** and –98.3, –46.1 cm^{-1} for **2**, respectively. The structural features indicate a higher magnitude of anitiferromagnetic coupling in the alkoxo-bridged unit based on the greater value of the Cu–O–Cu angle in comparison to the diphenoxo-bridged unit. The core structures of **1** and **2** compare well with the first generation model complexes for the active site structure of multicopper oxidases in the oxidized form. The crystal structure of **1** exhibits a lamellar structure with a gap of ∼7 Å containing water molecules in the interlamellar space. Complex **2** forms a hexanuclear species due to intermolecular hydrogen bonding interactions involving two trimeric units. The crystal packing diagram of **2** displays formation of a three-dimensional framework with cavities containing the perchlorate anions.

Introduction

Multicopper blue oxidases such as laccase, ascorbate oxidase, and ceruloplasmin catalyze the four-electron reduction of dioxygen to water.[1−6] The copper atoms present in these enzymes are of three types on the basis of their distinctly different EPR spectral features. The type-1 blue copper center shows an intense visible band near 600 nm

* To whom correspondence should be addressed. E-mail: arc@ipc.iisc.ernet.in.
[†] Department of Inorganic and Physical Chemistry.
[‡] Solid State and Structural Chemistry Unit.
[§] E-mail: ramasesh@sscu.iisc.ernet.in (for correspondence related to the theoretical part of the magnetic studies).

(1) Messerschmidt, A. *Struct. Bonding* **1998**, *90*, 37.
(2) Solomon, E. I.; Sundaram, U. M.; Machonkin, T. E. *Chem. Rev.* **1996**, *96*, 2563.
(3) Malkin, R.; Malmström, B. G. *Adv. Enzymol.* **1970**, *33*, 177.

10.1021/ic034565i CCC: $25.00
Published on Web 08/08/2003

Chart 1. Trinuclear Cores in the Active Site of Ascorbate Oxidase (a) and in the Model Complexes **1** and **2** Showing Atom Labeling for the Atoms in the Coordination Spheres along with the Proposed Magnetic Exchange Pathways ($J1$ and $J2$) (b)

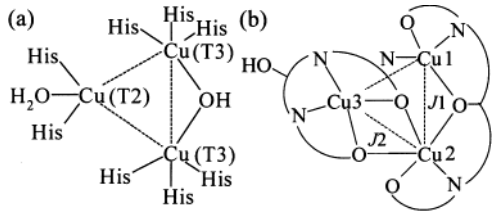

and a characteristic low $A_{||}$ value of $\sim 40-70 \times 10^{-4}$ cm^{-1} in the EPR spectrum. This site is found to be located at $\sim$12 Å from a trinuclear cluster consisting of a type-2 copper center ($A_{||} > 140 \times 10^{-4}$ cm^{-1}) and a coupled dinuclear type-3 copper center in the crystal structure of ascorbate oxidase.[7] The type-3 coppers are strongly antiferromagnetically coupled to make the dicopper(II) unit essentially diamagnetic and EPR undetectable. The trinuclear unit is proposed to be the active site for binding and multielectron reduction of dioxygen (Chart 1).[8] The crystal structure of ascorbate oxidase shows a triangular arrangement of the copper centers giving an average Cu···Cu distance of 3.74 Å in the oxidized form. It has a pair of copper atoms (putative T3) in which each copper shows coordination to three histidines and one bridging hydroxide giving a four-coordinate structure. The type-2 site has two histidines and an aqua ligand to make it three-coordinate. The fully reduced form of ascorbate oxidase also retains the trinuclear core but with an increase in the Cu···Cu distance of the putative type-3 site (5.1 Å), giving Cu···Cu distances between the type-2 and type-3 copper sites as 4.1 and 4.4 Å. The role of the type-1 copper is electron transfer to the type-3 coppers of the trinuclear active site through the His506-Cys507-His508 amino acid sequence segment in ascorbate oxidase.

The triangular core of multicopper oxidases has generated a lot of interest in the synthesis of low molecular weight trinuclear copper complexes having structural features similar to those of the active sites.[9,10] A majority of the reported trinuclear copper(II) complexes have, however, a linear geometry of the metal ions or a $Cu_3(\mu_3\text{-X})$ unit (X = Cl, OH).[11−14] In contrast, the number of angular trinuclear copper(II) complexes reported in the literature as "first generation" models for the active site of multicopper oxidases is limited.[15−30] The core structure and the magnetic properties of the majority of such model complexes differ considerably from those of the active site structure. The present work stems from our interest for a rational synthesis of a trinuclear core by covalent linkage of a type-2 mimic mononuclear copper(II) and a type-3 mimic dinuclear copper(II) complexes (Scheme 1). We have been successful in preparing tricopper(II) species from a reaction in which $[Cu(HL)](ClO_4)$ (**I**) and $[Cu_2L(\mu\text{-Br})]$ (**II**) in the presence of an imidazole base (L′) combine to form a trinuclear copper(II) core through two phenoxo bridges. The trinuclear core which shows the presence of a moderately strong antiferrromagnetically (AF) coupled dicopper(II) unit (type-3 mimic) and a relatively less AF-coupled unit is of importance toward modeling the active site structure of the multicopper oxidases (Chart 1). Herein, we report the synthesis, crystal structures, and magnetic properties of $[Cu_3(HL)L(Him)](ClO_4)$ (**1**) and $[Cu_3(HL)L(1\text{-MeIm})](ClO_4)$ (**2**), where H_3L is a pentadentate Schiff base ligand derived from salicylaldehyde and 1,3-diaminopropan-

(4) (a) Solomon, E. I.; Baldwin, M. J.; Lowery, M. D. *Chem. Rev.* **1992**, *92*, 521. (b) Solomon, E. I.; Lowery, M. D. *Science* **1993**, *259*, 1575.
(5) (a) Cole, J. L.; Clark, P. A.; Solomon, E. I. *J. Am. Chem. Soc.* **1990**, *112*, 9534. (b) Shin, W.; Sundaram, U. M.; Cole, J. L.; Zhang, H. H.; Hedman, B.; Hodgson, K. O.; Solomon, E. I. *J. Am. Chem. Soc.* **1996**, *118*, 3202. (c) Machonkin, T. E.; Solomon, E. I. *J. Am. Chem. Soc.* **2000**, *122*, 12547.
(6) Klinman, J. P. *Chem. Rev.* **1996**, *96*, 2541.
(7) (a) Messerschmidt, A.; Ladenstein, R.; Huber, R.; Bolognesi, M.; Avigliano, L.; Petruzzelli, R.; Rossi, A.; Finazzi-Agró, A. *J. Mol. Biol.* **1992**, *224*, 179. (b) Messerschmidt, A.; Rossi, A.; Ladenstein, R.; Huber, R.; Bolognesi, M.; Gatti, G.; Marchesini, A.; Petruzzelli, R.; Finazzi-Agró, A. *J. Mol. Biol.* **1989**, *206*, 513. (c) Messerschmidt, A.; Luecke, H.; Huber, R. *J. Mol. Biol.* **1993**, *230*, 997.
(8) (a) Allendorf, M. D.; Spira-Solomon, D. J.; Solomon, E. I. *Proc. Natl. Acad. Sci. U.S.A.* **1985**, *82*, 3063. (b) Spira-Solomon, D. J.; Allendorf, M. D.; Solomon, E. I. *J. Am. Chem. Soc.* **1986**, *108*, 5318. (c) Cole, J. L.; Tan, G. O.; Yang, E. K.; Hodgson, K. O.; Solomon, E. I. *J. Am. Chem. Soc.* **1990**, *112*, 2243.
(9) Fenton, D. E.; Okawa, H. *J. Chem. Soc., Dalton Trans.* **1993**, 1349.
(10) Cole, A. P.; Root, D. E.; Mukherjee, P.; Solomon, E. I.; Stack, T. D. P. *Science* **1996**, *273*, 1848.
(11) Some selected citations are the following: (a) Colacio, E.; Ghazi, M.; Kivekas, R.; Moreno, J. M. *Inorg. Chem.* **2000**, *39*, 2882. (b) Fernandes, C.; Neves, A.; Bortolussi, A. J.; Szpoganics, B.; Schwingel, E. *Inorg. Chem. Commun.* **2001**, *4*, 354. (c) Pasini, A.; Demartin, F.; Pioveseena, O.; Chiari, B.; Cinti, A.; Crispu, O. *J. Chem. Soc., Dalton Trans.* **2000**, 3467.
(12) (a) Ferrer, S.; Haasnoot, J. G.; Reedijk, J.; Miller, E.; Cingi, M. B.; Lanfranchi, M.; Lanfredi, A. M. M.; Ribas, J. *Inorg. Chem.* **2000**, *39*, 1859. (b) Root, D. E.; Henson, M. J.; Machonkin, T.; Mukherjee, P.; Stack, T. D. P.; Solomon, E. I. *J. Am. Chem. Soc.* **1998**, *120*, 4982.
(13) Kodera, M.; Tachi, Y.; Kita, T.; Kobushi, H.; Sumi, Y.; Kano, K.; Shiro, M.; Koikawa, M.; Tokii, T.; Ohba, M.; Okawa, H. *Inorg. Chem.* **2000**, *39*, 226.
(14) (a) Escuer, A.; Vicente, R.; Penalba, E.; Solans, X.; Font-Bardia, M. *Inorg. Chem.* **1996**, *35*, 248. (b) Van Albada, G. A.; Mutikainen, I.; Roubean, O. S.; Turpeinen, Y.; Reedijk, J. *Eur. J. Inorg. Chem.* **2000**, 2179 and selected references therein.
(15) Gehring, G.; Fleischhauer, P.; Paulus, H.; Haase, W. *Inorg. Chem.* **1993**, *32*, 54.
(16) Karlin, K. D.; Gan, Q.-F.; Farroq, A.; Liu, S.; Zubieta, J. *Inorg. Chem.* **1990**, *29*, 2549.
(17) Adams, H.; Bailey, N. A.; Dwyer, M. J. S.; Fenton, D. E.; Hellier, P. C.; Hempstead, P. D.; Latour, J.-M. *J. Chem. Soc., Dalton Trans.* **1993**, 1207.
(18) Chaudhuri, P.; Karpenstein, I.; Winter, M.; Butzlaff, C.; Bill, E.; Trautwein, A. X.; Flörke, U.; Haupt, H. J. *J. Chem. Soc., Chem. Commun.* **1992**, 321.
(19) Meenakumari, S.; Tiwary, S. K.; Chakravarty, A. R. *Inorg. Chem.* **1994**, *33*, 2085.
(20) Graham, B.; Spiccia, L.; Fallon, G. D.; Hearn, M. T. W.; Mabbs, F. E.; Moubaraki, B.; Murray, K. S. *J. Chem. Soc., Dalton Trans.* **2001**, 1226.
(21) Chaudhuri, P.; Winter, M.; Della Védova, B. P. C.; Bill, E.; Trautwein, A.; Gehring, S.; Fleischhauer, P.; Nuber, B.; Weiss, J. *Inorg. Chem.* **1991**, *30*, 2148.
(22) Epstein, J. M.; Figgis, B. N.; White, A. H.; Willis, A. C. *J. Chem. Soc., Dalton Trans.* **1974**, 1954.
(23) Pajunen, A.; Kivekas, R. *Cryst. Struct. Commun.* **1979**, *8*, 385.
(24) Bernhardt, P. V.; Hayes, E. J. *J. Chem. Soc., Dalton Trans.* **1998**, 3539.
(25) Colacio, E.; Dominguez-vera, J. M.; Escuer, A.; Klinga, M.; Kivekas, R.; Romerosa, A. *J. Chem. Soc., Dalton Trans.* **1995**, 343.
(26) Frey, S. J.; Sun, H. H. J.; Murthy, N. N.; Karlin, K. D. *Inorg. Chim. Acta* **1996**, *242*, 329.
(27) Wang, S. *Acta Crystallogr.* **1996**, *52C*, 41.
(28) Bertrand, J. A.; Marabella, C. P.; Vanderveer, D. G. *Inorg. Chim. Acta* **1977**, *25*, L69.
(29) Knuttila, H. *Inorg. Chim. Acta* **1983**, *72*, 11.
(30) Sanmartin, J.; Bermejo, M. R.; Garcia-Deibe, A. M.; Piro, O.; Castellano, E. E. *Chem. Commun.* **1999**, 1953.

Scheme 1[a]

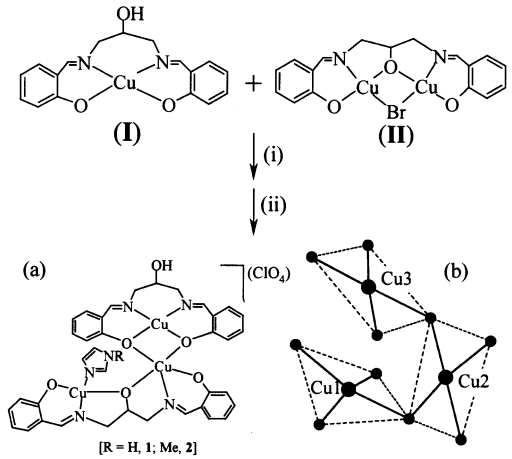

(a) Reaction conditions: MeOH−MeCN (1:1), reflux, 1.0 h; (i) imidazole or 1-methyl imidazole; (ii) $NaClO_4$; (b) relative orientations of the basal planes in the trinuclear core.

2-ol. The complexes show chemically significant hydrogen bonding interactions forming a lamellar structure of **1** and a framework structure with cavities for **2**.

Experimental Section

Materials and Measurements. All reagents and chemicals were purchased from commercial sources and used without further purification. The Schiff base *N*,*N*'-(2-hydoxypropane-1,3-diyl)bis-(salicylaldimine) (H_3L) and the copper(II) complex [Cu(HL)] were prepared by a literature procedure.[31] The dinuclear complex [Cu_2L-(μ-Br)] was prepared using a synthetic method reported for an analogous complex.[32] The elemental analyses were done using a Heraeus CHN-O Rapid instrument. The electronic and infrared spectral data were obtained from Hitachi U-3400 and Bruker Equinox 55 spectrometers, respectively. Electrochemical measurements were made at 25 °C on an EG&G PAR model 253 Versa Stat potentiostat/galvanostat with electrochemical analysis software 270 for cyclic and differential pulse voltammetric techniques using a three electrode setup comprising a glassy carbon working electrode, platinum wire auxiliary electrode, and a saturated calomel reference (SCE) electrode. The electrochemical data were uncorrected for junction potentials. Tetrabutylammonium perchlorate (TBAP) was used as supporting electrolyte. Ferrocene was used as a standard showing the Fe(III)/Fe(II) couple at 0.38 V (vs SCE) under similar experimental conditions in MeCN containing 0.1 M TBAP. Conductivity measurements were made at 25 °C using a Control Dynamics conductivity meter with a 10^{-3} M MeCN solution of the complexes.

Preparation of [Cu_3(HL)L(HIm)](ClO_4) (1). A 0.3 g (0.6 mmol) quantity of [Cu_2L(μ-Br)] in 10 mL of MeCN was added to a 10 mL MeOH solution of 0.22 g (0.6 mmol) of [Cu(HL)]. The mixture was heated to reflux for 10 min. A 0.04 g (0.6 mmol) quantity of imidazole was added to the solution that was refluxed further for a period of 1 h followed by addition of a 0.09 g (0.7 mmol) quantity of $NaClO_4$ taken in 5 mL of MeOH. The solution was cooled to an ambient temperature. Slow evaporation of the solvent gave a dark green solid of **1** in 0.45 g yield (~78%). The solid was isolated, washed with aqueous methanol and diethyl ether, and finally dried under vacuum over P_4O_{10}. Anal. Calcd for $C_{37}H_{35}N_6O_{10}ClCu_3$: C, 46.79; H, 3.71; N, 8.85. Found: C, 47.08; H, 3.98; N, 8.63. FT-IR, cm^{-1} (KBr phase): 3606 (br), 3425 (br), 3324 (br), 1638 (s), 1620 (s), 1537 (m), 1483 (m), 1445 (s), 1345 (m), 1303 (m), 1200 (w), 1117 (m), 1085 (s), 1064 (s), 971 (w), 900(w), 870 (w), 751 (m), 653 (w), 623 (m), 544 (w), 465 (w), 415 (w) [br, broad; s, strong; m, medium; w, weak].

Preparation of [Cu_3(HL)L(1-MeIm)](ClO_4) (2). This complex was prepared in ~75% yield by following the procedure already described using 0.05 mL of 1-methylimidazole (0.6 mmol) instead of imidazole. Anal. Calcd for $C_{38}H_{37}N_6O_{10}ClCu_3$: C, 47.35; H, 3.87; N, 8.72. Found: C, 47.12; H, 3.95; N, 8.60. FT-IR, cm^{-1} (KBr phase): 3437 (br), 1626 (s), 1605 (m), 1556 (w), 1536 (m), 1466 (m), 1442 (s), 1411(w), 1343 (w), 1302 (s), 1215 (w), 1203 (w), 1151 (m), 1110 (s), 1050 (m), 986 (w), 956(w), 891 (w), 856 (w), 804(w), 760 (s), 656 (w), 624 (m), 569 (w), 544 (w), 465 (w).

Safety Note. *Perchlorate salts of metal complexes with organic ligands are potentially explosive! Only small quantities of material should be prepared, and this should be handled with great caution.*

Magnetic Measurements. Variable temperature magnetic susceptibility data for the polycrystalline samples of **1** and **2** were obtained in the temperature range 18−300 K using model 300 Lewis Coil Force magnetometer (George Associates Inc., Berkeley, CA), equipped with a closed cycle cryostat (Air Products) and a Cahn balance. Hg[Co(NCS)$_4$] was used as a calibrant. Experimental susceptibility data were corrected for diamagnetic contributions and for temperature-independent paramagnetism (N_α).

As complexes **1** and **2** are paramagnetic with odd number of spin-$^1/_2$ ions, we used a model Hamiltonian in the presence of an applied magnetic field, *H*, as

$$\hat{H} = -J_1(\hat{S}_1\hat{S}_2) - J_2(\hat{S}_2\hat{S}_3) + gH\sum\hat{S}_i^z - zJ'\langle S^z_{tot}\rangle\sum\hat{S}_i^z \quad (1)$$

where the Heisenberg exchange constants, *J*s, are all negative since the interactions are all antiferromagnetic, *z* is the number of nearest neighbors of the complex in the crystal, $\langle S^z_{tot}\rangle$ is the mean magnetization of the complex, and $\hat{S}$s are the appropriate spin operators. To obtain the magnetic susceptibility in this model, we assumed that the intermolecular exchange constant J' is weak,[33] and following this model, we obtained the mean square magnetization of the isolated complex, $\langle M^2(T)\rangle$

$$M^2(T) = [\sum_i M_i^2 \exp(-E_i^{(0)}/k_BT)]/[\sum_i \exp(-E_i^{(0)}/k_BT)] \quad (2)$$

where T is the temperature and $E_i^{(0)}$ values are the energy eigenvalues of the isolated complex obtained by exact diagonalization of the Hamiltonian of the isolated complex in zero magnetic field. The magnetic susceptibility expression used for the complex in the crystal, within the molecular field approximation is then given by

$$\langle\chi(T)\rangle = -gM^2T/[k_BT - zJ'M^2(T)] \quad (3)$$

where the gyromagnetic ratio of the Cu atom is taken to be 2.00, the free electron value. To account for the possibility of a trace concentration of paramagnetic impurity present in the analytically pure sample, an additional Curie-like contribution to the susceptibility was assumed, so that $\chi_{tot}(T) = M/H + C/T$, where C is the Curie constant. The experimental curve was fit with different values of J_1 and J_2 (vide Chart 1b). The theoretical model gave good fitting with the experimental results. The error (R) calculated as $R = \sum_i[(\chi_{obs}(T_i) - \chi_{cal}(T_i))^2/\chi_{obs}(T_i)^2]$ was found to be 5.5×10^{-3} and 7.55

(31) Kitajima, N.; Whang, K.; Moro-oka, Y.; Uchida, A.; Sasada, Y. *J. Chem. Soc., Chem. Commun.* **1986**, 1504.
(32) Mazurek, W.; Berry, K. J.; Murray, K. S.; O'Connor, M. J.; Snow, M. R.; Wedd, A. G. *Inorg. Chem.* **1982**, *21*, 3071.
(33) Kahn, O. *Molecular Magnetism*; VCH: Weinheim, Germany, 1993.

$\times 10^{-3}$ for **1** and **2**, respectively. The Curie constants corresponded to a negligible impurity concentration of 0.4% in both **1** and **2**. Values of zJ' were -1.24 and -0.85 cm^{-1} for **1** and **2** indicating insignificant antiferromagnetic nature of intermolecular interaction.

X-ray Crystallographic Procedures for $[Cu_3(HL)L(HIm)](ClO_4)\cdot 1.5H_2O$ and $[Cu_3(HL)L(1\text{-}MeIm)](ClO_4)\cdot 0.5MeCN\cdot 0.5H_2O$. Single crystals of **1** were obtained by slow evaporation of the mother liquor of the complex. A crystal of approximate size $0.54 \times 0.38 \times 0.05$ mm^3 was mounted on a glass fiber using epoxy cement. The X-ray diffraction data were measured in frames with increasing ω (width of 0.3°/frame) at a scan speed of 8 s/frame using a Bruker SMART APEX CCD diffractometer, equipped with a fine focus sealed tube X-ray source. The SMART software was used for data acquisition and the SAINT software for data extraction. Empirical absorption corrections were made on the intensity data.[34] The structure was solved by the heavy atom method and refined by full-matrix least-squares using the SHELX system of programs.[35] All non-hydrogen atoms of the complex cation were refined anisotropically. Few hydrogen atoms were located from the difference Fourier map, and the rest were generated, assigned isotropic thermal parameters, and refined using a riding model. The hydrogen atoms were used for structure factor calculation only. There was a perchlorate anion in the asymmetric unit. The chlorine atom was refined anisotropically. The oxygen atoms showed high thermal motions, and they were refined isotropically using the SADI provision of the SHELX program for a tetrahedral structure of the anion. The Cl−O distances ranged from 1.36 to 1.40 Å. Besides this anion, there were solvent molecules in the asymmetric unit. While one peak was refined for a full occupancy water molecule, the other peak was located at a special position (x, y, z: 1.0, 0.0, 0.5). This peak was refined for an oxygen atom with a site occupancy factor of 0.5. As this water molecule belonged to two adjacent asymmetric units, in total there were 1.5 H_2O molecules per trimeric complex. The solvent oxygen atoms were refined isotropically. The structure refinement gave a goodness-of-fit (GOF) value of 0.97 with the maximum shift/esd value of 0.003. The highest peak in the final difference Fourier map showed an electron density of 1.187 e/Å^3 located 0.8 Å from the atom O(14) of the perchlorate anion.

Single crystals of complex **2** were grown from a solution of the complex in a MeCN−MeOH mixture (1:1 v/v) on slow evaporation of the solvent at 25 °C. A crystal of dimensions $0.39 \times 0.16 \times 0.06$ mm^3 was mounted on a glass fiber with epoxy cement, and the diffraction data were obtained from a Bruker SMART APEX CCD diffractometer at 100(2) K using a scan speed of 10 s/frame with increasing ω (width of 0.3° per frame). Empirical absorption corrections on the intensity data were made.[34] The structure of **2** was determined in a similar way as described for **1**. All non-hydrogen atoms of the complex and the perchlorate anion were refined anisotropically. Some hydrogen atoms were located from the difference Fourier map, and the rest were generated. They were refined by riding model and used for structure factor calculation only. The highest peak in the final difference Fourier map was 0.9 e/Å^3. Besides those for the complex and the perchlorate anion, there were three peaks in the final difference Fourier map showing electron density greater than 1.0 e/Å^3. One peak was assigned as oxygen with half site occupancy to get an acceptable thermal parameter. This peak was found to generate another peak in the adjacent asymmetric unit giving a distance of only 1.134 Å. The modeling was based for one water molecule positionally disordered in two adjacent asymmetric units. There were two more peaks in the difference Fourier map showing a distance of 1.683(4) Å from each other. One of them was found to be in a special position (x, y, z: 0.5, −0.0061, 0.25) with an occupancy factor of 0.5 as required by the symmetry. The other peak (x, y, z: 0.4986, −0.0123, 0.1876) was found to generate a peak by symmetry in the adjacent asymmetric unit giving a linear geometry. These peaks were modeled for an MeCN molecule belonging to two asymmetric units. The formulation gave 0.5 MeCN per complex molecule. The atom at the special position was refined as a carbon atom. The other peak was also refined as carbon although it should actually be 1:1 carbon and nitrogen with a site occupancy of 0.5 each. The goodness-of-fit (GOF) and the maximum shift/esd values were 0.883 and 0.002, respectively. Selected crystallographic data are presented in Table 1. Perspective views of the molecules were obtained using ORTEP.[36]

Table 1. Crystallographic Data for $[Cu_3(HL)L(HIm)](ClO_4)\cdot 1.5H_2O$ [**1**·1.5H_2O] and $[Cu_3(HL)L(1\text{-}MeIm)](ClO_4)\cdot 0.5MeCN\cdot 0.5H_2O$ [**2**·0.5MeCN·0.5H_2O]

	1·1.5H_2O	**2**·0.5MeCN·0.5H_2O
empirical formula	$C_{37}H_{38}N_6O_{11.5}ClCu_3$	$C_{39}H_{39.5}N_{6.5}O_{10.5}ClCu_3$
fw	976.8	993.34
cryst size, mm^3	$0.54 \times 0.38 \times 0.05$	$0.39 \times 0.16 \times 0.06$
cryst syst	monoclinic	monoclinic
space group	$P2_1/c$ (No. 14)	$C2/c$ (No. 15)
a, Å	13.884(3)	14.180(5)
b, Å	19.224(4)	23.932(5)
c, Å	14.829(3)	23.635(5)
β, deg	97.925(3)	95.280(5)
V, Å^3	3919.9(13)	7987(4)
Z	4	8
μ(Mo Kα), cm^{-1}	17.51	17.19
ρ_{calcd}, g cm^{-3}	1.655	1.652
λ, Å	0.71073	0.71073
T, K	293(2)	100(2)
R1[a] [R1 (all data)]	0.0666 [0.1678]	0.0736 [0.1279]
wR2[b] [wR2 (all data)]	0.1264 [0.1913]	0.1997 [0.1706]

[a] $R1 = \sum||F_o| - |F_c|/\sum|F_o|$. [b] $wR2 = \{\sum[w(F_o^2 - F_c^2)^2]/\sum[w(F_o^2)^2]\}^{1/2}$. $w = 1/[\sigma^2(F_o^2) + (AP)^2 + 0.0P]$ where $P = [\max(F_o^2, 0) + 2F_c^2]/3$, [$A$ = 0.1032 (**1**); 0.0658 (**2**)].

Results and Discussion

Synthesis and General Properties. Complexes **1** and **2** are prepared in high yield from the reaction of a monomeric type-2 mimic copper(II) complex (**I**) with a dimeric type-3 mimic copper(II) species (**II**) in the presence of an imidazole base and isolated as perchlorate salts (Scheme 1). The monomeric copper(II) complex, *N*,*N*'-(2-hydroxyproapane-1,3-diyl)bis(salicylaldiminato)copper(II), with a CuN_2O_2 coordination is known to model galactose oxidase (type-2 copper protein) activity by effectively catalyzing oxidation of primary alcohols in the presence of KOH and O_2.[31] The hydroxy group of the 1,3-diaminopropan-2-ol does not show any interaction with the metal atom in this monomeric complex. Dinuclear copper(II) complexes of such multidentate ligands have been used extensively to model the structural and functional properties of type-3 copper proteins, for NLO applications, and for deriving magneto-structural correlations.[32,37−40] The model complexes having an endogenous alkoxo or phenoxo bridging group mediate antiferro-

(34) Blessing, R. H. *Acta Crystallogr.* **1995**, *51A*, 33.
(35) Sheldrick, G. M. *SHELX-97, Programs for Crystal Structure Solution and Refinement*; University of Göttingen: Göttingen, Germany, 1997.
(36) Johnson, C. K. *ORTEP*; Report ORNL-5138; Oak Ridge National Laboratory: Oak Ridge, TN, 1976.

Table 2. Physicochemical Data for Complexes **1** and **2**

	1	**2**
IR, $\nu(ClO_4^-)$,[a] cm^{-1}	1085	1100
UV−vis, λ_{max}, nm (ϵ, $M^{-1}\,cm^{-1}$)[b]	607 (360); 364 (19 400); 272 (43 600)	607 (365); 364 (17 800); 272 (40 000)
μ_{eff}/μ_B, 300 K	2.98[c] (1.72)[d]	3.03[c] (1.75)[d]
μ_{eff}/μ_B, 18 K	2.1[c] (1.22)[d]	2.13[c] (1.23)[d]
Λ_M (mho $cm^2\,M^{-1}$)[e]	118	120
CV, $E_{1/2}$,V [ΔE_P, mV; i_{pa}/i_{pc}][f]	−0.99 [126; 0.8]	−0.97 [110; 0.8]

[a] KBr phase. [b] In MeCN, 10^{-3} M solution at 25 °C. [c] Value per Cu_3 unit. [d] Value per Cu. [e] Conductivity in MeCN. [f] Cyclic voltammetry using 10^{-3} M solution of the complexes in MeCN, 0.1 M TBAP; $E_{1/2} = 0.5(E_{pc} + E_{pa})$, where E_{pc} and E_{pa} are cathodic and anodic peak potentials, respectively; $\Delta E_p = (E_{pc} - E_{pa})$; i_{pa} and i_{pc} are anodic and cathodic peak currents, respectively. Scan rate: 50 mV s^{-1}.

magnetic coupling between two copper(II) centers thus making the singlet as the ground state. We have chosen the type-2 and type-3 mimic precursor complexes for the synthesis of a trinuclear core that can model the active site structure of multicopper oxidases. Complexes **1** and **2** are characterized by analytical and spectral methods. Relevant physicochemical data are given in Table 2. The 1:1 electrolytic complexes show characteristic perchlorate stretching bands in the IR spectra and display a d−d band at 607 nm in the electronic spectra in MeCN. Cyclic voltammetry of the complexes in MeCN containing 0.1 M TBAP using a glassy carbon working electrode exhibits a quasireversible voltammogram near −1.0 V giving an anodic to cathodic peak current ratio (i_{pa}/i_{pc}) of ∼0.8. The voltammetric response is assignable to the $Cu_3(II)/Cu_2(II)Cu(I)$ couple.

Crystal Structures. Complexes **1** and **2** are characterized by single-crystal X-ray diffraction technique. Selected bond distances and angles are given in Table 3. ORTEP diagrams of the complexes are shown in Figures 1 and 2. The structure of the cationic complexes consists of a trinuclear copper(II) core in which the monomeric type-2 mimic precursor complex (**I**) forms a covalent linkage with the dinuclear type-3 mimic complex (**II**) through two phenoxo oxygens belonging to the monomeric species (**I**) (Scheme 1). The removal of the exogenous bromide bridging ligand of the dimeric precursor has resulted in the binding of the phenoxo oxygen atoms of the monomer (**I**) to one copper center of the dimeric precursor. The imidazole ligand binds at the equatorial site of the other copper of the dimeric unit thus satisfying the coordination requirement of this copper atom. The Cu(1) and Cu(3) atoms in **1** and **2** have four-coordinate geometry. The Cu(1)···O(6) distances of 3.129(5) and 3.212(5) Å in **1** and **2** indicate no axial interaction involving the O(6) atom. The Cu(2) atom displays a five-coordinate

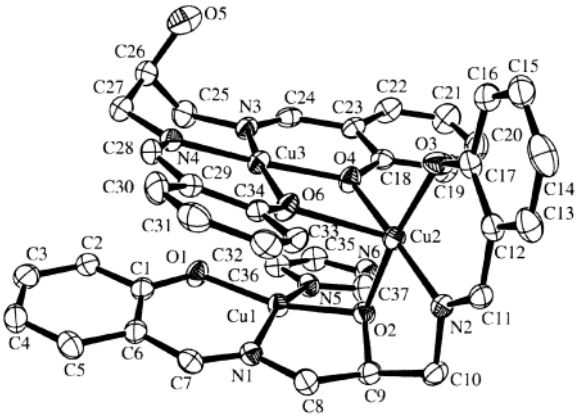

Figure 1. ORTEP view of the complex cation in $[Cu_3(HL)L(HIm)](ClO_4)\cdot 1.5H_2O$ (**1**·$1.5H_2O$) showing 30% probability thermal ellipsoids and the atom numbering scheme.

Table 3. Selected Bond Distances (Å) and Bond Angles (deg) in Complexes **1** and **2**

	1	**2**
Cu(1)···Cu(2)	3.286(1)	3.438(2)
Cu(2)···Cu(3)	3.283(1)	3.202(1)
Cu(1)−O(1)	1.906(5)	1.915(6)
Cu(1)−O(2)	1.940(4)	1.963(5)
Cu(1)−N(1)	1.949(6)	1.918(6)
Cu(1)−N(5)	1.962(6)	1.959(7)
Cu(2)−O(2)	1.975(4)	1.957(5)
Cu(2)−O(3)	1.911(5)	1.913(6)
Cu(2)−O(4)	2.016(4)	2.070(5)
Cu(2)−O(6)	2.344(5)	2.217(5)
Cu(2)−N(2)	1.931(5)	1.948(7)
Cu(3)−O(4)	1.982(5)	1.940(5)
Cu(3)−O(6)	1.902(4)	1.918(6)
Cu(3)−N(3)	1.957(6)	1.968(7)
Cu(3)−N(4)	1.988(6)	1.966(7)
Cu(1)−O(2)−Cu(2)	114.1(2)	122.5(3)
O(1)−Cu(1)−O(2)	160.8(2)	175.5(2)
O(1)−Cu(1)-N(1)	94.6(2)	92.9(3)
O(1)−Cu(1)−N(5)	93.4(2)	90.7(3)
O(2)−Cu(1)−N(1)	84.0(2)	84.0(3)
O(2)−Cu(1)−N(5)	93.4(2)	92.3(3)
N(1)−Cu(1)−N(5)	162.6(2)	176.3(3)
Cu(2)−O(4)−Cu(3)	110.4(2)	105.9(2)
Cu(2)−O(6)−Cu(3)	100.8(2)	101.3(2)
O(2)−Cu(2)−O(3)	170.5(2)	176.9(2)
O(2)−Cu(2)−O(4)	89.45(19)	92.9(2)
O(2)−Cu(2)−O(6)	96.03(17)	90.5(2)
O(3)−Cu(2)−O(4)	92.04(19)	89.9(2)
O(3)−Cu(2)−O(6)	93.3(2)	91.5(2)
O(4)−Cu(2)−O(6)	68.84(17)	70.9(2)
O(2)−Cu(2)−N(2)	84.1(2)	84.5(3)
O(3)−Cu(2)−N(2)	93.5(2)	92.4(3)
O(4)−Cu(2)−N(2)	171.9(2)	155.7(2)
O(6)−Cu(2)−N(2)	116.7(2)	133.1(2)
O(4)−Cu(3)−O(6)	79.30(19)	80.4(2)
O(4)−Cu(3)−N(3)	90.5(2)	92.6(3)
O(4)−Cu(3)−N(4)	169.1(2)	163.3(2)
O(6)−Cu(3)−N(3)	169.1(2)	170.9(3)
O(6)−Cu(3)−N(4)	92.5(2)	91.0(3)
N(3)−Cu(3)−N(4)	98.1(2)	97.2(3)

(4 + 1) geometry with a relatively short Cu(2)−O(6) axial bond distance. This axial bond in **1** is relatively longer than in **2** ($\Delta d = 0.13$ Å). The Cu(2)−O(4) bond lengths in **1** and **2** are marginally different ($\Delta d = 0.04$ Å). A shorter Cu(2)−O(4) bond length in **1** has resulted in lengthening of the Cu(3)−O(4) distance ($\Delta d = 0.04$ Å). The Cu(3)−O(6), Cu(3)−N(3), and Cu(3)−N(4) distances are essentially same in both the complexes. The Cu(2)−O(6)−Cu(3) angles are

(37) (a) Blackman, A. G.; Tolman, W. B. *Struct. Bonding* **2000**, *97*, 179. (b) Neves, A.; Rossi, L. M.; Vencato, I.; Drago, V.; Haase, W.; Werner, R. *Inorg. Chim. Acta* **1998**, *281*, 111. (c) Karlin, K. D.; Kaderli, S.; Zuberbühler, A. *Acc. Chem. Res.* **1997**, *30*, 139. (d) Kitajima, N.; Moro-oka, Y. *Chem. Rev.* **1994**, *94*, 737.
(38) Nishida, Y.; Kida, S. *J. Chem. Soc., Dalton Trans.* **1986**, 2633.
(39) Fernandes, C.; Neves, A.; Bortoluzzi, A. J.; Mangrich, A. S.; Rentschler, E.; Szpoganicz, B.; Schwingel, E. *Inorg. Chim. Acta* **2001**, *320*, 12.
(40) (a) Averseng, F.; Lacroix, P. G.; Malfant, I.; Périssé, N.; Lepetit, C.; Naketani, K. *Inorg. Chem.* **2001**, *40*, 3797. (b) Ku, S.-M.; Wu, C.-Y.; Lai, C. K. *J. Chem. Soc., Dalton Trans.* **2000**, 3491.

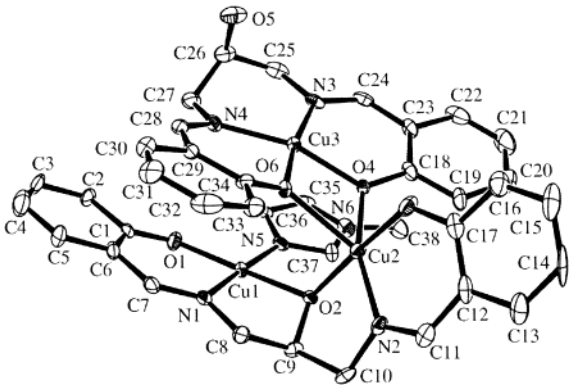

Figure 2. ORTEP view of the cationic complex in $[Cu_3(HL)L(1\text{-MeIm})](ClO_4)\cdot 0.5MeCN\cdot 0.5H_2O$ (**2**·0.5MeCN·0.5H$_2$O) displaying 30% probability thermal ellipsoids and the atom labeling scheme.

Table 4. Deviation of Copper Atoms from the Basal Planes (d) and Dihedral Angles between the Basal Planes (φ) for the Coordination Geometries in **1**·1.5H$_2$O and **2**·0.5MeCN·0.5H$_2$O with esd Values Given in the Parenthesis

	1	**2**
	d Values (Å)	
Cu(1)	0.057(2)	0.040(1)
Cu(2)	0.126(2)	0.192(1)
Cu(3)	0.033(1)	0.081(1)
	Dihedral Angles[a] (φ, deg)	
plane1−plane2	82.2(2)	69.0(2)
plane2−plane3	87.1(2)	77.0(2)

[a] Basal planes 1−3 contain Cu(1)−Cu(3) atoms, respectively.

similar, but the Cu(2)−O(4)−Cu(3) angles differ by ∼4°. The basal Cu(2)−N(2) and Cu(2)−O(3) and the alkoxo bridging Cu(2)−O(2) distances are also similar in both the structures. The Cu(1) atom in a CuN_2O_2 coordination shows similar structural features in both **1** and **2**. The trianionic ligand exhibits a pentadentate mode of bonding to Cu(1) and Cu(2) with an endogenous alkoxide bridge giving a Cu(1)−O(2)−Cu(2) angle of 114.1° in **1** and 122.5° in **2**.

The covalent linkage of the type-2 mimic and type-3 mimic precursors has resulted in the formation of a triangular core. The deviation of the metal atoms from the basal planes and the dihedral angles between two basal planes are given in Table 4. The Cu(1)N_2O_2 unit is essentially planar in **2** showing the Cu(1) atom displaced by 0.04 Å from the plane. This same plane in **1** is significantly distorted although the copper atom shows a minor deviation of 0.06 Å from the plane. The observed difference could be related to the lower Cu(1)−O(2)−Cu(2) bite angle in **1** in comparison to **2**. The planarity of the basal unit of Cu(2) atom also differs in **1** and **2**. The four donor atoms form a plane with the copper atom 0.13 Å above the plane in **1**. A similar plane calculation for **2** shows significant distortion displaying O(2) and O(3) atoms below and N(2) and O(4) atoms above the plane. The Cu(2) atom is displaced 0.19 Å from the plane. The Cu(2)−O(6) axial bond length in **1** is significantly longer than in **2**. The Cu(3)N_2O_2 unit is essentially planar in **1** showing a displacement of the Cu(3) atom of 0.03 Å from the plane. The same unit in **2** shows significant distortion from planarity with the Cu(3) atom displaced by 0.08 Å from the plane. The dihedral angles between N(3)−Cu(3)−O(4) and N(4)−Cu(3)−O(6) planes are 7.6° in **1** and 14.6° in **2**. A much larger tetrahedral distortion from the square-planar geometry is reported for the crystal structure of the precursor complex [Cu(HL)] (**I**) showing a dihedral angle between two O−Cu−N planes as 35.7°.[31] The six-membered rings having the propan-2-ol moiety display an envelope conformation, and the hydroxy group does not show any significant interaction with the copper.

The phenoxo oxygen atoms O(4) and O(6) within the trinuclear core bridge the Cu(2) and Cu(3) atoms. The sum of the angles at O(4) and O(6) atoms in **1** and **2** is ca. 360°. Both the phenoxo oxygen atoms thus have a planar geometry. The dihedral angle between two basal planes containing the Cu(2) and Cu(3) atoms is ∼80° in the complexes. The O(6) atom shows equatorial/axial binding mode. The plane containing Cu(2), Cu(3), O(4), and O(6) atoms is essentially planar. The alkoxo bridging oxygen O(2) has a pyramidal geometry as the sum of the angles at O(2) is 332° in **1** and 335° in **2**. The dihedral angle between the basal planes containing Cu(1) and Cu(2) atoms is 82° in **1** and 69° in **2**. The Cu(1)···Cu(2) and Cu(2)···Cu(3) distances in **1** are 3.286(1) and 3.283(1) Å, respectively. The same distances in **2** are 3.438(2) and 3.202(1) Å. The Cu···Cu distances in the complexes are shorter than the av Cu···Cu distance of 3.74 Å in the active site of ascorbate oxidase. The Cu(1)···Cu(3) spatial separation is 3.158(2) Å in **1** and 3.327(2) Å in **2**. The Cu···Cu···Cu angles in the triangular cores of **1** and **2** range between 56.48(3)° and 63.50(3)°.

The complexes form two significantly different types of three-dimensional network structures due to hydrogen bonding interactions involving the hydroxy group of the 1,3-diaminopropan-2-ol moiety, the imidazole proton, the lattice water, and the perchlorate anion. The distance between the O(5) and O(7) atoms in **1** is 2.861(6) Å [O(5)−H(5A)···O(7), 148.6(4)°]. The imidazole NH proton in **1** is involved in a hydrogen bonding interaction with the O(14) atom of the perchlorate anion belonging to another asymmetric unit [N(6)···O(14)$^{\#1}$, 2.941 Å; N(6)−H(6)···O(14)$^{\#1}$, 155.3(5)°; #1: $-x, -1/2 + y, 1/2 - z$]. The crystal packing diagram of complex **1** shows the formation of a lamellar structure with a gap of ∼7 Å containing water molecule in the interlamellar space (Figure 3). Complex **2** shows intermolecular hydrogen bonding interactions to form an unprecedented hexanuclear species involving the hydroxy group of the propan-2-ol moiety of the Schiff base and a terminal phenoxo oxygen of another trinuclear unit [O(5)···O(3)$^{\#2}$, 2.773(8) Å; O(5)−H(5A)···O(3)$^{\#2}$, 171.9(5)°; #2: $-x, -y, -z$] (Figure 4). The O(7) atom of the lattice water is hydrogen bonded with the O(14) atom of the perchlorate anion [O(7)···O(14), 2.387(13) Å]. The crystal packing diagram of **2** displays the formation of cavities of diameters varying from ∼11 to ∼4 Å containing the perchlorate anions (Figure 5).

A comparison of the structural results of **1** and **2** with the reported "first generation" model complexes having an angular arrangement of the tricopper(II) core has been made in Table 5.[15−30] The core units of the majority of the triangular copper(II) model complexes differ considerably from the active site structure. Among the reported ones, only

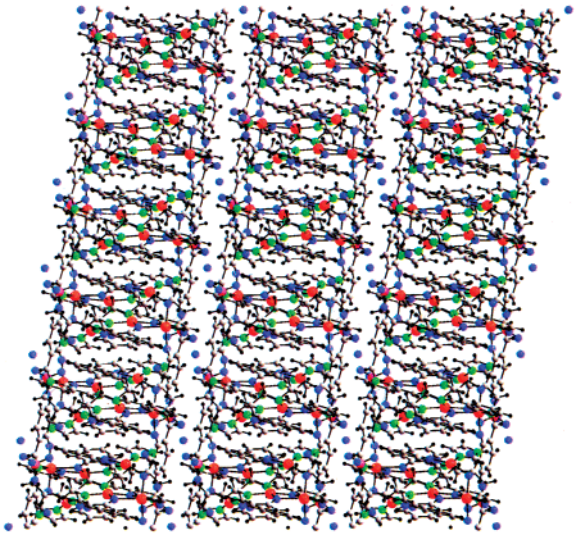

Figure 3. Crystal packing diagram of $[Cu_3(HL)L(HIm)](ClO_4)\cdot 1.5H_2O$ along *b*-axis showing the formation of lamellar structure with lattice water molecules in the interlamellar region (Cu, red; Cl, pink; O, blue; N, green; C, gray; H, black).

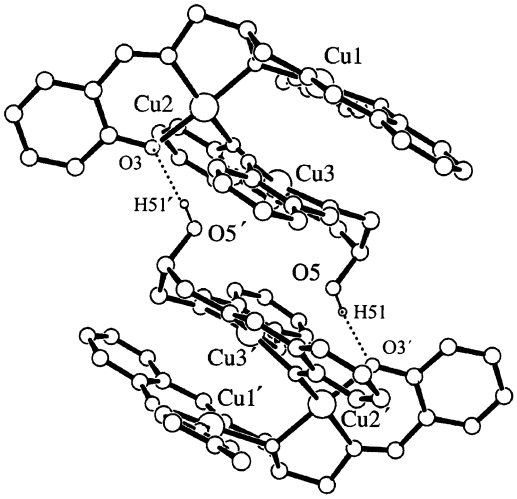

Figure 4. Formation of a discrete hexameric structure by intermolecular hydrogen bonding interactions in $[Cu_3(HL)L(1\text{-MeIm})](ClO_4)\cdot 0.5MeCN\cdot 0.5H_2O$.

two complexes, viz. $[Cu_3(OH)(L^1)(H_2O)](ClO_4)_3\cdot 2H_2O$ and $[Cu_3L^{mes}(OH)_2(H_2O)_2](ClO_4)_4\cdot 3.2H_2O$, have structural resemblance to the active site structure.[17,20] These structures, however, show significantly long distances between the copper centers belonging to type-3 and type-2 model sites.

Magnetic Properties. The variable temperature magnetic susceptibility data in the temperature range 300−18 K show an antiferromagnetic behavior of **1** and **2**. Both the complexes have nearly the same μ_{eff} values of ∼3.00 μ_B at 300 K and ∼2.0 μ_B at 18 K. The variable temperature magnetic susceptibility curves, shown in Figures 6 and 7, display a gradual decrease of the susceptibility on lowering the temperature with a plateau near 26 K giving a magnetic moment of 1.9 μ_B per tricopper unit that corresponds to one unpaired electron. A theoretical fit of the magnetic data for the complexes has been made using an antiferromagnetic spin-$^1/_2$ Heisenberg model for the trinuclear core. The model assumes two exchange parameters, viz. J_1, for the Cu(1), Cu(2) pair, and J_2, for the Cu(2), Cu(3) pair of copper ions and neglects the Cu(1), Cu(3) interaction based on the geometry of the complexes (Chart 1b).

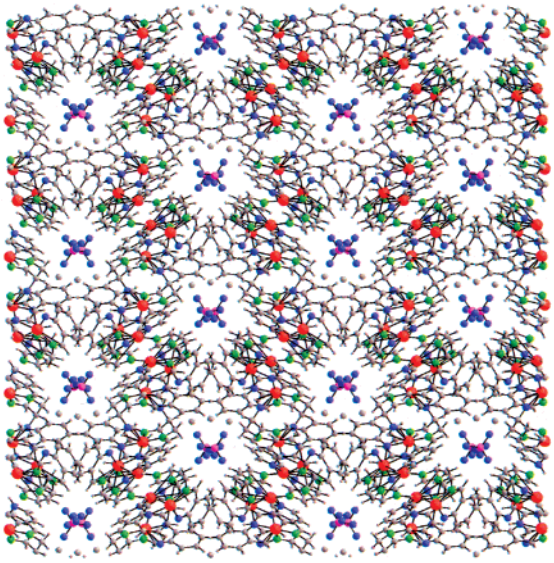

Figure 5. Crystal packing diagram of $[Cu_3(HL)L(1\text{-MeIm})](ClO_4)\cdot 0.5MeCN\cdot 0.5H_2O$ showing formation of cavities containing the perchlorate anions (Cu, red; Cl, pink; O, blue; N, green; C and H gray).

Table 5. Selected Model Complexes Having Angular Trinuclear Copper(II) Cores

Sl no.	complex	Cu···Cu, Å	$-J$ (cm^{-1})	ref
1	$[Cu_3L^1(OH)(H_2O)](ClO_4)_3\cdot 2H_2O$[a]	3.62; 5.89; 4.95	101	17
2	$[Cu_3(Me_3tacn)_3(Im)_3](ClO_4)_3$[b]	5.92	75	18
3	$[Cu_3(O_2CMe)_4(bpy)_3(H_2O)](PF_6)_2$[c]	3.20; 6.28; 4.57	−79; 0.2	19
4	$[Cu_3L^{mes}(OH)_2(H_2O)_2](ClO_4)_4\cdot 3.2H_2O$[d]	2.90	24	20
5	$[Cu_3(Me_3tacn)_2(dmg)_2Br]ClO_4\cdot MeOH$[b,e]	3.38; 6.56	224	21
6	$[Cu_3(HL^2)L^2(H_2O)Cl](ClO_4)_2\cdot 4.88H_2O$[f]	3.37; 4.77	189	25
7	$[Cu_3L^3(NO_3)_2(H_2O)_3](NO_3)_4\cdot 5H_2O$[g]	5.83; 6.24; 8.77		26
8	$[Cu_3(H_2L^4)L^4]\cdot 2H_2O$[h]	3.41; 3.86		30
9	$[Cu_3(HL)L(HIm)](ClO_4)\cdot 1.5H_2O$[i]	3.29; 3.28	82.7; 73	*k*
10	$[Cu_3(HL)L(1\text{-MeIm})](ClO_4)\cdot 0.5MeCN\cdot 0.5H_2O$[j]	3.44; 3.20	98.3; 46.1	*k*

[a] H_2L^1, bis(2,6-diacetyliminopyridino)-*N*,*N*′-bis{3-(2-salicylaldiminoethyl)-3-azapenta-1,5-diyl}. [b] Me$_3$tacn, 1,4,7-trimethyl-1,4,7-triazacyclononane. [c] Bpy, 2,2′-bipyridyl. [d] L^{mes}, 1,3,5-tris(1,4,7-triazacyclonon-1-ylmethyl)benzene. [e] Dmg, dimethylglyoxime dianion. [f] H_2L^2, *N*,*N*′-bis(1,3-dimethyl-5-nitrosopyrimidine-2,4(1*H*,3*H*)-dion-6-yl)propylenediamine. [g] L^3, *N*,*N*,*N*′,*N*′,*N*″,*N*″-{hexakis(2-pyridylmethyl)}tris(2-aminoethyl)amine. *J* value not available. [h] H_4L^4, *N*,*N*′-(butane-1,4-diyl)bis(3-hydroxysalicylaldimine). *J* value not available. [i] H_3L, *N*,*N*′-(2-hydoxypropane-1,3-diyl)bis(salicylaldimine). [i]HIm, imidazole. [j] 1-MeIm, 1-methylimidazole. [k] This work.

In **1**, the alkoxo-bridge angle is 114.1(2)°. The Cu(1)−O(2) and Cu(2)−O(2) distances are ∼1.96 Å. These two copper atoms are linked by one oxygen atom. For the other pair of metal ions, viz. Cu(2) and Cu(3), connected through O(4), the mean Cu−O(4) distance is 2.00 Å and the Cu(2)−O(4)−Cu(3) phenoxo-bridge angle is 110.4°. In both these cases, the $d_{x^2-y^2}$ orbitals of the copper ions are involved on either side of the bridging oxygen, and the nature of exchange interaction is antiferromagnetic. In structure **1**, there appears to exist another exchange pathway for the Cu(2), Cu(3) pair of copper atoms, through the O(6) atom. However, magnetic exchange through the O(6) atom would involve the singly

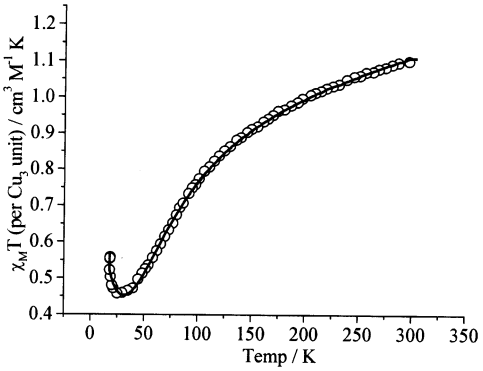

Figure 6. $\chi_M T$ vs T plot for $[Cu_3(HL)L(HIm)](ClO_4)\cdot 1.5H_2O$ (**1**). The circles are the experimental points, and the solid line is the theoretical fit of the experimental data.

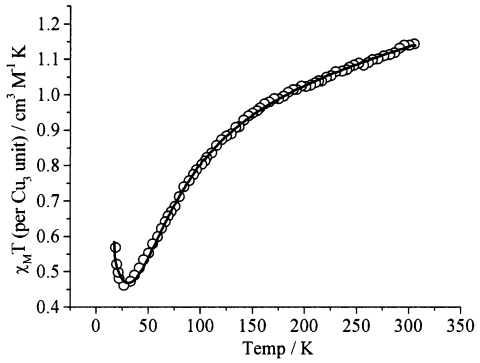

Figure 7. Temperature dependence of $\chi_M T$ plot for $[Cu_3(HL)L(1\text{-MeIm})](ClO_4)$ (**2**) along with the theoretical fit (solid line) to the experimental data.

occupied $d_{x^2-y^2}$ orbital of Cu(3) atom and the doubly occupied d_{z^2} orbital of the Cu(2) atom, and the exchange interaction would be negligible. From the structure, we also note that there is no exchange pathway between the Cu(1) and Cu(3) atoms. Thus, a microscopic model Hamiltonian for describing the magnetism in this system would involve two exchange parameters. Assuming that the magnitude of the Heisenberg exchange constants depends on the Cu−O−Cu bond angle θ as $\cos(\theta)$, the exchange constants J_1 for the Cu(1)−Cu(2) pair and J_2 for the Cu(2)−Cu(3) pair should be in the ratio 1.17:1. This provides a valuable guide while fitting the experimental susceptibility versus temperature plots to a microscopic model. For **2**, the alkoxo-bridge angle connecting the Cu(1) and Cu(2) copper atoms is 122.5(3)°. The Cu(1)−O(2) and Cu(2)−O(2) distances are both ∼1.96 Å. For the other pair of copper atoms, viz. Cu(2) and Cu(3) as in **1**, only the phenoxo bridge is important, and the bond angle for this bridge, Cu(2)−O(4)−Cu(3), is 105.9(2)°. The Cu(2)−O(4) and the Cu(3)−O(4) distances are also nearly equal with the average Cu−O(4) distance being 1.97 Å. The Cu(1)−Cu(3) pair does not have a viable exchange pathway. Following the same arguments as for **1**, we would expect the two exchange constants J_1 and J_2 to be in the ratio 1.96:1. The coupling constants J_1 and J_2, obtained from the theoretical fit of the susceptibility data, are −82.7 and −73 cm^{-1} for **1**, and −98.3 and −46.1 cm^{-1} for **2**. The ratio of J_1 and J_2 is 1.13:1 for **1** and 2.13:1 for **2**, values which are in reasonable agreement with the expected ratio mentioned previously based on simple arguments.

Within the tricopper(II) core, the magnitude of antiferromagnetic interaction is expected to be more for the alkoxo-bridged copper pair (J_1) than the diphenoxo-bridged dicopper unit (J_2). The mono-hydroxo/alkoxo-bridged dicopper(II) complexes having a Cu−O−Cu angle in the range 130−145° are known to be strongly AF-coupled.[17,20,32,38,41] The precursor dinuclear complex with a $Cu_2(\mu\text{-Br})(\mu\text{-OR})^{2+}$ core shows an antiferromagnetic coupling giving a J value of −49 cm^{-1}. An analogous complex having a $Cu_2(\mu\text{-Cl})(\mu\text{-OR})^{2+}$ core, where the alkoxide bridge is from a pentadentate ligand derived from the condensation of salicylaldehyde and 1,5-diaminopentan-3-ol (2:1 ratio), the intramolecular antiferromagnetic coupling parameter (J) is known to be −53 cm^{-1}.[42] The alkoxo-bridged dicopper(II) unit in **1** and **2** is, however, better related to the $Cu_2(\mu\text{-OR})^{3+}$ core in $[Cu_2(L^5)(OMe)(MeOH)]$, where H_3L^5 is a pentadentate Schiff base obtained from 1,3-diaminopropan-2-ol and methylacetoacetate.[38] The magnitude of the AF coupling parameter (J) in the L^5 complex having a Cu−O−Cu angle of 137.7° is −317.5 cm^{-1}. In contrast, the magnitude of J_1 in **1** and **2** is moderately low. One possible reason could be the pyramidal geometry of the O(2) atom, that could reduce the extent of AF interaction in comparison to a planar structure of the oxygen atom.[42] The pyramidal geometry of the O(2) atom has also resulted in lowering the Cu(1)−O(2)−Cu(2) bond angle.

The Cu(2) and Cu(3) atoms are linked by O(4) and O(6) phenoxide atoms. This Cu_2O_2 unit is essentially planar, and the oxygen atoms have a planar geometry. The magnetic study of dinuclear complexes with a planar $[Cu_2(\mu\text{-OH})_2]^{2+}$ core has received considerable attention for deriving magneto-structural correlations.[33,43,44] Hodgson and Hatfield have put forward a correlation between the exchange coupling constant (J) and the Cu−O−Cu angle (θ) as $2J = -74.53\theta + 7270$ cm^{-1}.[43] In **1** and **2**, the mean Cu(2)−O−Cu(3) angle is ∼104°. If we use the Hatfield correlation, a $2J$ value of ∼ −450 cm^{-1} is expected for this $Cu_2(\mu\text{-OR})_2^{2+}$ core. The observed values are significantly less considering the large value of θ angle. In addition to the planarity of the core, the

(41) (a) Burk, P. L.; Osborn, J. A.; Youinou, M. T.; Agnus, Y.; Louis, R.; Weiss, R. *J. Am. Chem. Soc.* **1981**, *103*, 273. (b) Coughlin, P. K.; Lippard, S. J. *J. Am. Chem. Soc.* **1981**, *103*, 3228. (c) Haddad, S. R.; Wilson, S. R.; Hodgson, D. J.; Hendrickson, D. N. *J. Am. Chem. Soc.* **1981**, *103*, 384. (d) Drew, M. G. B.; McCann, M.; Nelson, J. *J. Chem. Soc., Dalton Trans.* **198**1, 1868. (e) McKee, V.; Smith, J. *J. Chem. Soc., Chem. Commun.* **1983**, 1465. (f) Thompson, L. K.; Harstock, F. W.; Robichaud, P.; Hanson, A. W. *Can. J. Chem.* **1984**, *62*, 2755. (g) Thompson, L. K.; Lee, F. L.; Gabe, E. J. *Inorg. Chem.* **1988**, *27*, 39.

(42) Mazurek, W.; Kennedy, B. J.; Murray, K. S.; O'Connor, M. J.; Rodgers, J. R.; Snow, M. R.; Wedd, A. G.; Zwack, P. R. *Inorg. Chem.* **1985**, *24*, 3258.

(43) Crawford, V. H.; Richardson, H. W.; Wasson, J. R.; Hodgson, D. J.; Hatfield, W. E. *Inorg. Chem.* **1976**, *15*, 2107.

(44) (a) Chaudhuri, P.; Ventur, D.; Wieghardt, K.; Peters, E.-M.; Peters, K.; Simon, A. *Angew. Chem., Int. Ed. Engl.* **1985**, *24*, 57. (b) Charlot, M. F.; Jeannin, S.; Jeannin, Y.; Kahn, O.; Lucrece-Aubal, J.; Martin, J. S. *Inorg. Chem.* **1979**, *18*, 1675. (c) Charlot, M. F.; Kahn, O.; Jeannin, S.; Jeannin, Y. *Inorg. Chem.* **1980**, *19*, 1410. (d) Graham, B.; Hearn, M. T. W.; Junk, P. C.; Kepert, C. M.; Mabbs, F. E.; Moubaraki, B.; Murray, K. S.; Spiccia, L. *Inorg. Chem.* **2001**, *40*, 1536.

dihedral angle of ~80° between two basal planes containing the Cu(2) and Cu(3) atoms is expected to alter the magnitude of the J_2 parameter. Kida and co-workers[45] have studied the effect of structural factors on magnetism of di-μ-alkoxodicopper(II) complexes. The theoretical results demonstrated that the Cu−O−Cu angle has the major effect on the *J*-value. Other factors such as the dihedral angle between two coordinate planes, planarity of bonds on the bridging oxygens, tetrahedral distortion of the coordination planes, and the tilt of O−C bond of the alkoxide bridge from the O−O axis are less effective on the magnitude of the *J*-parameter. The observation of a higher magnitude of AF coupling parameter (J_2) for **1** in comparison to **2** is related to the greater value of the Cu(2)−O(4)−Cu(3) angle in **1** than in **2**. Again, the $[Cu_2(\mu\text{-}OR)_2]^{2+}$ core in **1** can be considered to be effective as $[Cu_2(\mu\text{-}OR)]^{3+}$ unit due to the long Cu(2)−O(6) distance. The same core in **2** can be treated as $[Cu_2(\mu\text{-}OR)_2]^{2+}$. The Cu(2)−O(6)−Cu(3) angle remains essentially the same in both **1** and **2**. The theoretical work of Kida et al. predicts a variation of *J* as $|\Delta J|$/deg of 7.4 cm^{-1}. The $\Delta\theta$ value of **1** and **2** considering the Cu(2)−O(4)−Cu(3) angle of the complexes is ~4.5°. This predicts a $|\Delta J|$ value of 33.3 cm^{-1}. The observed $|\Delta J_2|$ value is 29.6 cm^{-1}.

Magnetic properties of selected first generation model complexes having an angular trinuclear core are compared in Table 5. The complex containing the L^1 ligand has an antiferromagnetically coupled $Cu_2(\mu\text{-}OH)^{3+}$ unit as a type-3 mimic and an essentially uncoupled copper(II) center.[17] A similar core structure is also reported for the bpy and L^{mes} complexes, each having a coupled dicopper(II) unit and an isolated copper(II) center. However, they do not model the active site magnetically. While the tricarboxylato-bridged dicopper(II) core is ferromagnetic in the bpy complex,[19] the $Cu_2(\mu\text{-}OH)^{2+}$ core is weakly antiferromagnetically coupled in the L^{mes} species.[20] Besides, the Cu···Cu distance in the $Cu_2(\mu\text{-}OH)^{2+}$ unit of L^{mes} complex is only 2.9 Å which is much shorter than the Cu···Cu distance of 3.74 Å of the active site. The Cu···Cu distances between the type-3 mimic and type-2 mimic copper centers are significantly longer than 3.74 Å in these model complexes. Again, complexes $[Cu_3(Me_3tacn)_3(Im)_3]^{3+}$ and $[Cu_3(Me_3tacn)_2(dmg)_2Br]^{+}$ show significantly different structural features and magnetic properties in comparison to the trinuclear active site. The cationic complex $[\{Cu(\mu\text{-}HL^2)Cu(H_2O)(\mu\text{-}L^2)Cu\}(\mu\text{-}Cl)]^{2+}$ has two Cu···Cu distances of 3.4 and 4.8 Å.[25] The core structure and its magnetic properties do not show any resemblance with the active site. The complex $[Cu_3(L^3)(NO_3)_2(H_2O)_3]^{4+}$ has a core which is unlikely to have any intramolecular spin-exchange interactions. The isosceles triangular core in $[Cu_3(H_2L^4)L^4]$ has two phenoxo bridges. The Cu(1)···Cu(2) and Cu(1)···Cu(1A) distances in the $\{Cu(1)(\mu\text{-}OR)Cu(2)(\mu\text{-}OR)Cu(1A)\}$ unit, where Cu(1)···Cu(1A) are symmetry related atoms, are 3.4 and 3.9 Å. The magneto-structural properties of **1** and **2** compare well with the first generation model complexes.

Conclusions

Two new trinuclear copper(II) complexes, viz. $[Cu_3(HL)L(HIm)](ClO_4)$ (**1**) and $[Cu_3(HL)L(1\text{-}MeIm)](ClO_4)$ (**2**), are prepared from a reaction of $[Cu(HL)]$ with $[Cu_2L(\mu\text{-}Br)]$ in the presence of imidazole bases. This work presents a synthetic procedure in which a monomeric type-2 mimic complex is covalently linked with a dinuclear type-3 mimic to form the angular trinuclear copper(II) complexes as models for blue copper oxidases. The Cu···Cu separation of ca. 3.3 Å in **1** and **2** is ~0.4 Å shorter than that in the active site structure. Within the core, the dicopper(II) unit having an endogenous alkoxide bridge shows a moderately strong antiferromagnetic interaction, thus retaining the type-3 magnetic behavior. The diphenoxo-bridged dicopper(II) unit mediates antiferromagnetic interaction but to a lesser extent in comparison to the alkoxide bridge. The terminal copper having the phenoxo bridging atoms partially retains the type-2 property. The role of imidazole base is to render stability to the structure by fulfilling the coordination requirement of one terminal copper atom.

Complexes **1** and **2** display novel hydrogen bonding interactions. Complex **1** form a lamellar structure with a 7 Å interlamellar gap containing the lattice water. Complex **2** forms a supramolecular structure with cavities of ~11 Å diameter containing the perchlorate anions. It also shows the formation of a discrete hexameric structure by intermolecular hydrogen bonding interactions. Among **1** and **2**, the latter presents a better magnetic model for the active site structure of blue copper oxidases by showing a ΔJ difference of 52.2 cm^{-1}. The synthetic methodology adopted for the preparation of **1** and **2** may be useful in fine-tuning the structural features to get more accurate magnetic models for the active site.

Acknowledgment. The authors thank the Department of Science and Technology, Government of India, for the financial support (SP/S1/F01/2000) and for the CCD diffractometer facility. Thanks are due to the Alexander von Humboldt Foundation, Germany, for the donation of an electroanalytical system, and the Bioinformatics Center of the Indian Institute of Science, Bangalore, for database search.

Supporting Information Available: Cyclic voltammograms of **2** in MeCN containing 0.1 M TBAP (Figure S1), plane calculations giving deviation values (*d*) of the atoms from the least-squares planes (Table S1), variable temperature magnetic susceptibility data for **1** and **2** (Tables S2 and S3), and a listing of full crystallographic data, atomic coordinates, full list of bond distances and bond angles, anisotropic thermal parameters, and hydrogen atom coordinates for complexes **1** and **2** in CIF format. This material is available free of charge via the Internet at http://pubs.acs.org.

IC034565I

(45) Handa, M.; Koga, N.; Kida, S. *Bull. Chem. Soc. Jpn.* **1988**, *61*, 6853.